

Simulating Ramsey-Type Fringes in a Pulsed Microwave-Driven Classical Josephson Junction

Jeffrey E. Marchese*

Department of Applied Science, University of California, Davis, California 95616, USA

Matteo Cirillo†

Dipartimento di Fisica, Università di Roma "Tor Vergata", I-00173 Roma, Italy

Niels Grønbech-Jensen‡

Department of Applied Science, University of California, Davis, California 95616, USA

(TQMFA05 November 2005, March 2006)

Abstract. We present evidence for a close analogy between the nonlinear behavior of a pulsed microwave-driven Josephson junction at low temperature and the experimentally observed behavior of Josephson systems operated below the quantum transition temperature under similar conditions. We specifically address observations of Ramsey-type fringe oscillations, which can be understood in classical nonlinear dynamics as results of slow transient oscillations in a pulsed microwave environment. Simulations are conducted to mimic experimental measurements by recording the statistics of microwave-induced escape events from the anharmonic potential well of a zero-voltage state. Observations consistent with experimentally found Ramsey-type oscillations are found in the classical model.

1. Introduction

Macroscopic quantum behavior of Josephson systems has been the focus of intense research over the past years due to the potential applications of Josephson technology in quantum information processing [1]. Many experimental observations have been conducted in order to characterize and understand the quantum properties of various Josephson device and networks [2, 3, 4, 5, 6, 7, 8, 9, 10, 11, 12]. Due to the nature of the Josephson effect it is not easy to make direct observations of the expected quantum states in the anharmonic potential of a zero-voltage state Josephson system, so most measurements are conducted statistically by recording the distributions of transitions from one system state to another. These transitions are commonly induced through the controlled application of microwaves and microwave pulses of frequencies that are commensurate with the expected energy

*Supported by the UC Davis Center for Digital Security, AFOSR grant FA9550-04-1-0171

†Supported by MIUR (Italy) COFIN04

‡Supported by the UC Davis Center for Digital Security, AFOSR grant FA9550-04-1-0171

separations between possible quantum levels of the system.

Some of the key microwave induced features that have been used to illustrate the quantum properties of Josephson systems are multi-peaked switching distributions as a function of bias-point in continuously applied microwaves [13, 14], observations of Rabi-oscillations [15] in the switching statistics of systems perturbed by pulsed microwaves [3, 7, 12], and the associated Ramsey-fringes[16] when several coordinated and parameterized microwave pulsed are applied sequentially [10, 11]. These observations, along with many others, have produced a large body of insight to the dynamical response of Josephson systems to microwave perturbations applied at very low temperature, and the acquired data has been used to interpret the quantum nature of the superconducting networks under investigation. However, many of the observations may also be attributed to classical nonlinear dynamics and statistics. For example, it has been demonstrated that the multi-peak switching distributions as a function of varying system bias for a constantly applied microwave field can be understood as classical high-Q resonances in the nonlinear system [14, 17]. Also Rabi-type oscillations in the switching statistics of Josephson systems perturbed by microwave pulses have been shown to be consistent with theoretical and numerical expectations based on a classical model of a Josephson junction, which exhibit the transients in response to the pulsed perturbations [18, 19]. It is the purpose of this paper to demonstrate that Ramsey-type fringes can also be observed in the classical model when the recipe of the experimental measurements is followed. We here, for simplicity, illustrate the results with the simplest possible system, namely a single classical Josephson junction, perturbed by a bias-current, microwave fields, probe fields, and thermal noise.

2. The Model

The normalized classical equation for a perturbed Josephson junction within the RCSJ model (see Figure 1a) is [20],

$$\ddot{\varphi} + \alpha\dot{\varphi} + \sin \varphi = \eta + \varepsilon_s(t) \sin(\omega_s t + \theta_s) + \varepsilon_p(t) + n(t), \quad (1)$$

where φ is the difference between the phases of the quantum mechanical wave functions defining the junction, η represents the dc bias current, and $\varepsilon_s(t)$, ω_s , and θ_s represent microwave amplitude, frequency, and phase, respectively (see Figure 1b). All currents are normalized to the critical current I_c , and time is measured in units of the inverse plasma frequency, ω_0^{-1} , where $\omega_0^2 = 2eI_c/\hbar C = 2\pi I_c/\Phi_0 C$, C being the capacitance of the junction, and $\Phi_0 = h/2e$ is the flux quantum. Tunneling of quasiparticles is represented by the dissipative term, where $\alpha = \hbar\omega_0/2eRI_c$ is given by the shunt resistance R , and the accompanying thermal fluctuations are defined by the dissipation-fluctuation relationship [21]

$$\langle n(t) \rangle = 0 \quad (2)$$

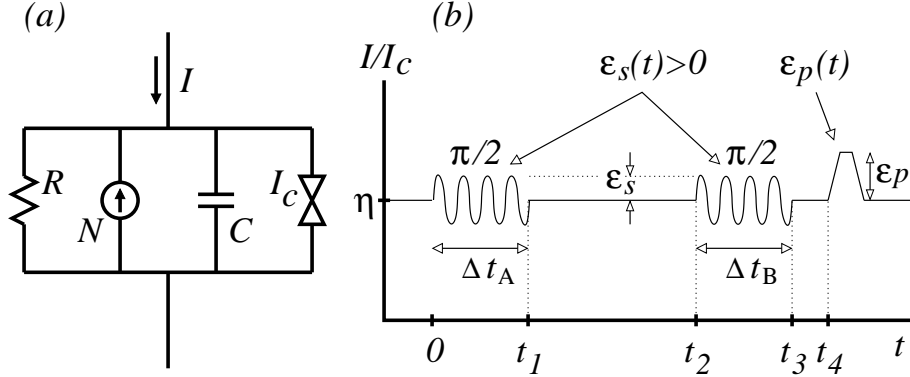


Fig. 1: (a) Sketch of the RCSJ model where $I/I_c = \eta + \varepsilon_s(t) \sin(\omega_s t + \theta) + \varepsilon_p(t)$ and $N = n(t)I_c$. (b) Sketch of the current supply to the junction.

$$\langle n(t)n(t') \rangle = 2\alpha \frac{k_B T}{H_J} \delta(t - t') = 2\alpha \Theta \delta(t - t'), \quad (3)$$

T being the thermodynamic temperature, H_J is the characteristic Josephson energy $H_J = I_c \hbar / 2e$, and Θ is thereby defined as the normalized temperature. A current pulse for probing the state of the system is represented by $\varepsilon_p(t)$.

3. Simulation Details

Following the procedure of reported experiments, we record the switching from the zero-voltage state ($\langle \dot{\varphi} \rangle = 0$) as a result of applying the external current sketched in Figure 1b. We first equilibrate the system at a chosen temperature for a given value of η . For a randomly chosen, but temporally constant, phase θ_s , a microwave pulse with frequency ω_s , which is associated with the natural resonance of the junction at bias point η , is applied for a duration of Δt_A . This duration is chosen to be $\Delta t_A = \tau_R / 4$, where $\tau_R = 2\pi / \Omega_R$ is the Rabi-type oscillation period [18, 19] for the microwave amplitude ε_s . This pulse is denoted a $\pi/2$ -pulse due to its parameterization based on Rabi-type oscillations. Another $\pi/2$ -pulse, in phase θ_s with the first pulse, is applied at a later time with identical amplitude, frequency, and duration ($\Delta t_B = \Delta t_A$), whereafter a short pulse $\varepsilon_p(t)$ is applied to probe whether the system is in a high or low energy state after the sequential microwave pulse application. The probe pulse is parameterized such that a state of relatively high system energy at t_3 will result in a likely escape event when $\varepsilon_p(t)$ is activated, while a state of relatively low system energy will result in a low probability of escape when $\varepsilon_p(t)$ is activated. This procedure is repeated many times,

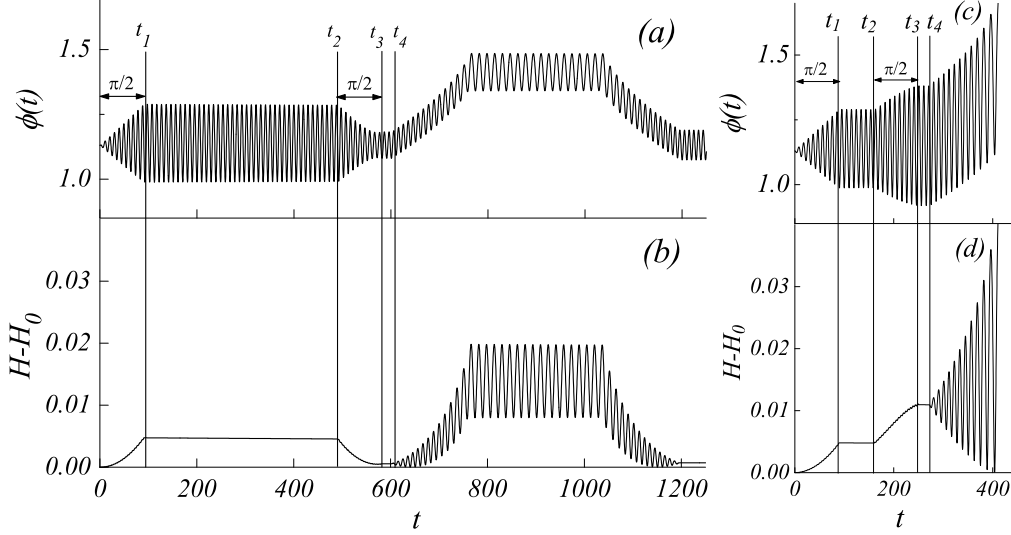


Fig. 2: Josephson response to the sequential application of two $\pi/2$ microwave pulses followed by a probe field. (a,c) Josephson phase. (b,d) System energy as defined by Equations (4) and (5). Parameters are $\alpha = 10^{-4}$, $\eta = 0.904706$, $\varepsilon_s = 2.17 \cdot 10^{-3}$, $\varepsilon_p = 8.2 \cdot 10^{-2}$, and $\Theta = 0$. (a,b) Non-switching for $\Delta t_d = t_2 - t_1 = 400$. (c,d) Switching for $\Delta t_d = t_2 - t_1 = 70$.

each time with a new realization of θ_s , in order to generate information about the probability of switching for a given set of parameters, such as the time delay between the two $\pi/2$ -pulses. Figure 2 illustrates typical examples of the events described above for $\Theta = 0$. Specific parameter values are: $\alpha = 10^{-4}$, $\varepsilon_s = 2.17 \cdot 10^{-3}$, $\varepsilon_p = 8.2 \cdot 10^{-2}$, $\omega_s = \omega_l$, and $\eta = 0.904706$, which results in a linear resonance frequency of $\omega_l = \sqrt[4]{1 - \eta^2} = 0.652714$. $\pi/2$ -pulses are applied in the intervals $t \in [0; t_1 = \Delta t_A]$ and $t \in [t_2; t_3 = t_2 + \Delta t_B]$ with $\Delta t_A = \Delta t_B = 90.75$ time units. This value is obtained from the corresponding Rabi-type oscillations reported in [19]. After the second $\pi/2$ -pulse, a short delay of $\Delta t = 20$ is allowed before the probe pulse $\varepsilon_p(t)$ is initiated at t_4 . The probe has linear rise and fall times of 160 normalized time units with a constant value interval of 275 time units. We show the system response to the microwave perturbations in terms of both phase φ and the normalized energy $H - H_0$, which is defined by

$$H = \frac{1}{2}\varphi^2 + 1 - \cos \varphi - \eta\varphi \quad (4)$$

$$H_0 = 1 - \sqrt{1 - \eta^2} - \eta \sin^{-1} \eta. \quad (5)$$

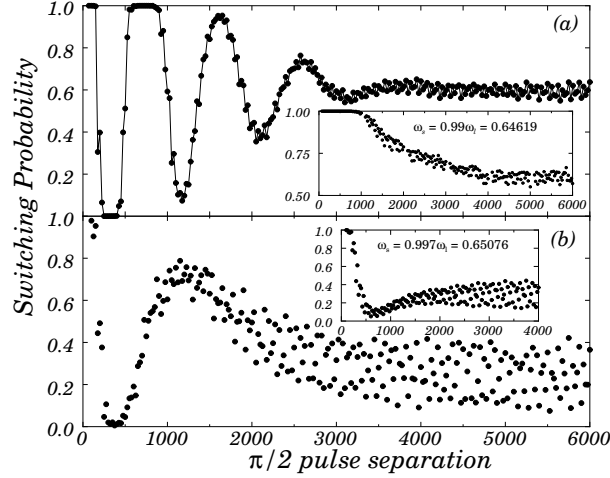


Fig. 3: Switching probability as a function of $\pi/2$ -pulse separation for $\Theta = 2 \cdot 10^{-4}$. Each point represents statistics of 2,500 events. Parameters are as in Figure 2, unless otherwise listed. (a) $\alpha = 10^{-4}$. Visible Ramsey-type fringe oscillation for $\omega_s = \omega_l = \sqrt[4]{1 - \eta^2} = 0.652714$. Inset shows vanishing Ramsey-type fringe frequency near $\omega_s = 0.990\omega_l$. (b) same as (a), except for $\alpha = 10^{-3}$. Inset shows vanishing Ramsey-type fringe frequency near $\omega_s = 0.997\omega_l$.

Figures 2a and 2b show the response for $\Delta t_d = 400$. It is evident that the first $\pi/2$ -pulse elevates the system energy by leaving the system in a phase-locked state at $t = t_2$ with energy $E(t_1)$. At the onset of the second $\pi/2$ -pulse, a significant phase-slip between the oscillation of φ and the microwave has developed during the interval $[t_1; t_2]$, and the second microwave pulse therefore decreases the energy of the Josephson system. The system is left at $t = t_3$ with energy $E(t_3) < E(t_1)$, which, when the probe field is applied at t_4 , results in only temporary energy increase while the probe is applied; this is not enough to make the system switch into a non-zero voltage state, which can be seen from the fact that $E(t) \rightarrow 0$ for large t . For comparison we show Figures 2c and d for $\Delta t_d = 70$. We here observe the same initial behavior, but the application of the second $\pi/2$ -pulse leaves the system in a relatively high energy state $E(t_3) > E(t_1)$, since the phase-slip between the junction and the microwave field is minor in this case. Consequently, the junction phase φ switches out of the bound state when the probe pulse is applied at t_4 . This is recognized by the diverging energy for $t > t_4$.

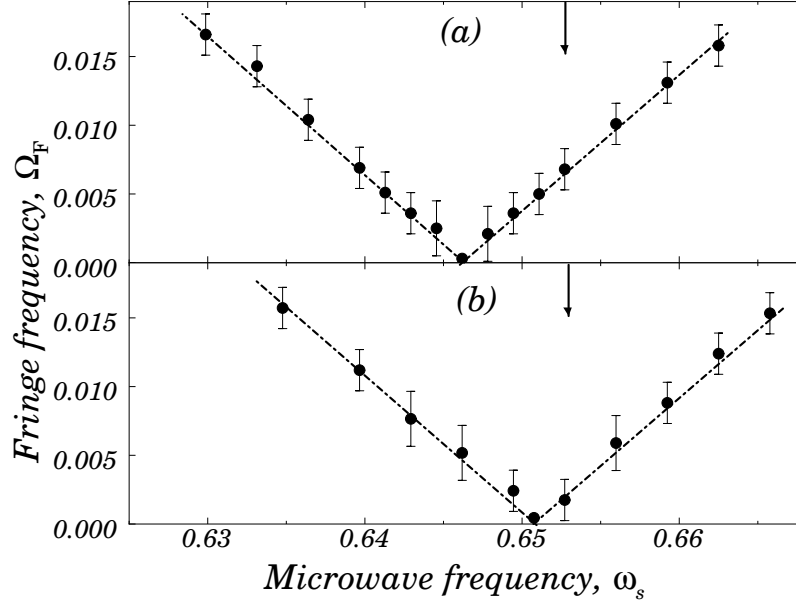


Fig. 4: Ramsey-type fringe frequency Ω_F as a function of applied microwave frequency for two different dissipation parameters: (a) $\alpha = 10^{-4}$, and (b) $\alpha = 10^{-3}$. Other parameters are as in Figure (3). Arrows indicate the driving frequency for which $\omega_s = \omega_l$. Dashed lines indicate a slope of ± 1 .

4. Ramsey-Type Fringes

Ramsey-type fringes in the switching probability as a function of $\pi/2$ -pulse separation can be directly observed in Figure 3, where we have shown the variation of the switching probability for $\Theta = 2 \cdot 10^{-4}$, calculated as averages of 2,500 events for different values of α and ω_s . Figure 3a clearly shows a distinct frequency, which we will name the Ramsey-type fringe frequency Ω_F , for $\omega_s = \omega_l = \sqrt[4]{1 - \eta^2} = 0.652714$ and $\alpha = 10^{-4}$. The inset shows that the fringe frequency depends on the applied microwave frequency such that $\omega_s = 0.990\omega_l$ results in $\Omega_F \approx 0$. Similar behavior is observed for larger dissipation parameter $\alpha = 10^{-3}$ shown in Figure 3b. Clearly, the fringe-frequency is different for $\omega_s = \omega_l$, compared to Figure 3a, and in this case $\omega_s = 0.997\omega_l$ results in $\Omega_F \approx 0$.

A number of simulations of the Ramsey-type fringe frequency for different microwave frequencies have been conducted, and the results are summarized in Figure 4, where the fringe frequency Ω_F is shown as a function of microwave frequency ω_s for the two different dissipation parameters mentioned in Figure 3. The vertical arrows indicate the linear resonance frequency $\omega_l = \sqrt[4]{1 - \eta^2}$. The simulation data are represented by markers with error bars. The frequencies are

read from figures like Figure 3. For low Ω_F , less than one wavelength of fringe oscillation may be visible and the oscillation may be somewhat distorted (see Figure 3b). In such cases we measured the time from the first trough (peak) to the next peak (trough) and used the half period to determine the frequency. In the case of saturation such as Figure 3a, we measured the period of the first regular waveform. These issues also account for some of the distortion in Figure 4.

We observe the distinct "V-shape" signature of the Ramsey-type frequency $\Omega_F(\omega_s)$ [10] with a slope very close to \pm unity (lines with slope ± 1 are shown in Figure 4 along with the simulation data), and $\Omega_F \approx 0$ for microwave frequencies close to ω_l . It is noticeable that the characteristic microwave frequency for which $\Omega_F = 0$ increases with α , and we further notice that this characteristic frequency is smaller than ω_l . While we have found no experimental data for comparison, future experiments may want to address this observation.

5. Conclusions

Like Rabi-type oscillations and resonant multi-peak switching distributions, Ramsey-type fringes have been used to identify and analyze expected macroscopic quantum behavior of Josephson systems. In this paper we have addressed the comparable classical system through direct simulations of the well-established nonlinear classical model equation, which is driven according to the recipe prescribed by the experimental reports of Ramsey-fringes. Our results show that even the simplest possible classical Josephson model, the single RCSJ model, clearly exhibits the features of Ramsey-type fringes when the model is used to simulate a low temperature, low dissipation system. A detailed theoretical analysis of classical Ramsey-type fringes [22] can be developed in close analogy with, and extension of, the analysis of phase-locking transients that have been found to be responsible for, e.g., Rabi-type oscillations in pulsed microwave-driven classical Josephson systems [18, 19].

6. Acknowledgment

We are grateful to A. V. Ustinov for several useful discussions.

Bibliography

1. *Quantum Computing and Quantum Bits in Mesoscopic Systems*, A. Leggett, B. Ruggiero, and P. Silvestrini, Eds. (Kluwer Academic/Plenum Publishers, New York, 2004).
2. D. Vion, A. Aasime, A. Cottet, P. Joyez, H. Pothier, C. Urbina, D. Esteve, and M. H. Devoret, *Science* **296**, 886 (2002).
3. J. M. Martinis, S. Nam, J. Aumentado, *Phys. Rev. Lett.* **89**, 117901 (2002).
4. D. Vion, A. Aasime, A. Cottet, P. Joyez, H. Pothier, C. Urbina, D. Esteve, and M. H. Devoret, *Fortschr. Phys.* **51**, 462 (2003).

5. J. M. Martinis, S. Nam, J. Aumentado, K. M. Lang, *Phys. Rev. B* **67**, 094510 (2003).
6. I. Chiorescu, Y. Nakamura, C. J. P. M. Harmans, J. E. Mooij, *Science* **299**, 1869 (2003).
7. J. Claudon, F. Balestro, F. W. J. Hekking, O. Buisson, *Phys. Rev. Lett.* **93**, 187003 (2004).
8. T. Kutsuzawa, H. Tanaka, S. Saito, H. Nakano, K. Semba, H. Takayanagi, *Appl. Phys. Lett.* **87**, 073501 (2005).
9. A. Wallraff, D. I. Schuster, A. Blais, L. Frunzio, J. Majer, M. Devoret, S. M. Girvin, R. J. Schoelkopf, *Phys. Rev. Lett.* **95**, 060501 (2005).
10. B. L. T. Plourde, T. L. Robertson, P. A. Reichart, T. Hime, S. Linzen, C. Wu, J. Clarke, *Phys. Rev. B* **72**, 060506 (2005).
11. R. H. Koch, J. R. Rozen, G. A. Keefe, F. M. Milliken, C. C. Tsuei, J. R. Kirtley, D. P. DiVincenzo, *Phys. Rev. B* **72**, 092512 (2005).
12. R. W. Simmonds, K. M. Lang, D. A. Hite, S. Nam, D. P. Pappas, and J. M. Martinis, *Phys. Rev. Lett.* **93**, 077003 (2004).
13. A. Wallraff, A. Lukashenko, A. V. Ustinov, *Phys. Rev. Lett.* **90**, 037003 (2003).
14. N. Grønbech-Jensen, M. G. Castellano, F. Chiarello, M. Cirillo, C. Cosmelli, L. V. Filippenko, R. Russo, and G. Torrioli, *Phys. Rev. Lett.* **93**, 107002 (2004).
15. I. I. Rabi, *Phys. Rev. Lett.* **51**, 652 (1937).
16. N. F. Ramsey, *Phys. Rev.* **78**, 695 (1950).
17. N. Grønbech-Jensen, M. G. Castellano, F. Chiarello, M. Cirillo, C. Cosmelli, V. Merlo, R. Russo, and G. Torrioli, in *Quantum Computing: Solid State Systems*, edited by B. Ruggiero, P. Delsing, C. Granata, Y. Paskin, and P. Silvestrini (Kluwer Academic/Springer Publishers, New York, 2005), cond-mat/0412692.
18. N. Grønbech-Jensen and M. Cirillo, *Phys. Rev. Lett.* **95**, 067001 (2005).
19. J. E. Marchese, M. Cirillo, N. Grønbech-Jensen, arXiv:cond-mat/0509729, (2005).
20. A. Barone and G. Paternò, *Physics and Applications of the Josephson Effect* (Wiley, New York 1982).
21. G. Parisi, *Statistical Field Theory* (Addison-Wesley, Redding, MA, 1988).
22. J. E. Marchese, M. Cirillo, N. Grønbech-Jensen, to be published.